

Particle Trajectories in the BBM Approximation

Olufemi Elijah Ige and Zahra Khorsand

Abstract—The regularized version of the KdV equation called the BBM equation has been used as a model equation for long waves in shallow water. This model is used to study the behavior of the waves at the surface of the inviscid fluid. In this paper, the particle paths are computed numerically with the aid of the velocity fields found in connection with the exact solutions of the BBM equation. In line with this concept, we examine the solitary wave and the periodic traveling wave solutions. For comparison purposes, we compute the closed-form solutions of the particle trajectories analytically.

Index Terms—BBM equation, surface wave, particle trajectories, solitary waves, periodic waves.

I. INTRODUCTION

THE Benjamin-Bona-Mahony (BBM) equation is one of the well known models for the study of surface waves. It proved very useful as far as real-life applications are concerned [1]. The BBM model integrates the nonlinearity and dispersive effects for the propagation of long waves. However, its applications are significant in the investigation of the long-wavelength in the liquids, hydromagnetic waves in cold plasma and acoustic waves in harmonic crystals [1]. Many works have been done by scientists since the discovery of this model.

For shallow-water waves, the BBM equation has proven to be the appropriate regularized form of the KdV equation in studying some characteristics and features embedded in water waves in rectangular channels [2]. It should be noted however, that in reality, river basins are not usually rectangular (see for example Fig. 3) in [3]. This model offers significant technical advantage over the KdV equation when the existence and stability are taken into consideration. In particular, the equation is contractive (see for example [4]). However, under the undeniable theoretical findings, the BBM equation has shown beyond doubt to be a high-quality model for long waves [5]. Besides being a shallow water model, its application in studying the drift waves or the Rossby waves is incredible. It also serves as a paradigm upon which a one-dimensional wave model is built under some specific conditions.

The linearized mathematical models for both KdV and BBM equations can serve as the platform on which the main mathematical contrast between these two equations can be most readily comprehended by juxtaposing their respective dispersion relation. [6], [7]. Understandably, these expressions are comparable for small wave numbers only, and they produce exceedingly distinct reactions to the short waves, this gives one of the justifications why the existence

and regularity theory for the KdV equation is demanding and comparatively simple for the BBM equation [8]. The BBM equation did not consider dissipation and is nonintegrable [9], [10], [11].

An enormous body of research work is ongoing purposely on finding the exact, solitary, and periodic traveling wave solutions of the BBM equation owing to the great significance of this equation [12]. However, much research that features the physical examination of internal and surface water waves has been studied using the BBM model. Diverse effective methods from a mathematical point of view have been used to study the exact, solitary, and periodic traveling wave solutions of the BBM model. Some of these methods include the homogeneous balance method by Abdel Rady et al. [13], the factorization technique by Estevez et al. [14], and the Jacobi elliptic function expansion method by An and Zhang [15]. Wave breaking has been studied using a BBM-type system for undular bores created by a moving weir in [16]. However, this setup is fairly different from the present situation. A situation which is more closely connected to the present setup is considered in [17], [18]. The aspect of the BBM equation being a model for the surface water waves, that is, the relationship between the surface water patterns and underlying flow is yet to be given a great deal of attention.

In this study, our focus will mainly be on the particle paths beneath the surface wave of a given fluid, and the BBM model as a governing equation will be investigated in the non-dimensional form

$$\eta_t + \eta_x + \frac{3}{2}\eta\eta_x - \frac{1}{6}\eta_{xxt} = 0, \quad (1)$$

which comes into limelight when the undisturbed depth h_0 is considered as a unit of distance, and $\sqrt{h_0/g}$ is deemed as a unit of time. The expression for the fluid velocity field beneath the surface can be remodeled from the derivation of the BBM equation as a surface water-wave model. Remarkably, the expressions for the vertical and horizontal velocity components as regards the unknown variable η , which describes the free surface structure can be derived. From our observation, it is easy to point out that to first order in the perturbation parameter, the depth at which the horizontal velocity u is measured is not associated with the said velocity, so we have $u = \eta$. However, forasmuch as the BBM equation is justifiable to second order, this expression may be refined to read

$$u = \eta - \frac{1}{4}\eta^2 + \frac{1}{3}\eta_{xx}, \quad (2)$$

which is valid to second-order [19]. In equation (2), u represents the horizontal velocity at the even bottom. However, obtaining an equation for the horizontal velocity at an arbitrary depth in the fluid column is feasible. This concept has been established implicitly in the derivation shown in [19], and it has also been used to the good advantage

Manuscript received January 08, 2020; revised April 22, 2020.

Olufemi Elijah Ige (corresponding author) is with the Department of Mathematics, University of Bergen, Postbox 7800, 5020 Bergen, Norway. (e-mail: olufemi.ige@uib.no).

Zahra Khorsand is with the Department of Mathematics, University of Bergen, Postbox 7800, 5020 Bergen, Norway. (e-mail: zahra.khorsand@gmail.com).

in the study of a general system of Boussinesq equations [20], [21]. Upon finding the velocity field associated with a surface wave, then it is possible to explore the dynamic properties embedded in the flow, especially, the approximate descriptions of the trajectories traced out by fluid particles underneath the surface may be constructed.

Since the BBM equation is well-founded asymptotically in the limit of small amplitude and long wavelength, it is expected that the results gotten are of approximate value, and its application should only be for waves of small amplitude, and long wavelength [22].

An immense body of research has emerged on particle paths since the discovery of solitary waves and periodic traveling-wave solutions. In the work carried out in [23], the particle trajectories connected to the solitary-wave solutions of the water-wave problem was studied by Constantin and Escher, they proved that in a solitary water wave each particle is transported in the wave direction but slower than the wave speed. Moreover, the qualitative results of the particle velocities and particle paths were proved using maximum principles for elliptic operators.

Particle paths in the linearized water-wave were studied by Constantin et al. [24] and Constantin and Villari [25], the study showed that these trajectories are not closed. These types of results are known as Stokes drift in engineering, they were presented in [24], [25] when mathematical authentications had not been in existence. In addition, Ehrnstrm and Villari evaluate the mathematical results on particle trajectories within steady two-dimensional water waves, in which the linear and exact mathematical theory of periodic and symmetric waves were prioritized [26]. Moreover, a numerical approach for finding the particle trajectories of nonlinear gravity waves in deep water waves was published by Chang et al. [27], this context was studied in the Lagrangian framework.

However, the velocity field below a solitary and periodic traveling wave can be approximated by using a direct approximation of the wave system, without performing the Boussinesq scaling [22]. For example, the higher-order approximations of solitary waves that permit the estimation of the velocity field beneath the surface are found by Fenton [28] and Grimshaw [29]. In [30], Chen et al. found to high accuracy, the particle trajectories due to periodic wave, and the results were compared to the experimental results observed in wave-tank.

The previous results which are in accordance with the present study were obtained by Borluk and Kalisch [22], they found the velocity fields which are connected to exact solutions of the KdV equation and constructed the particle paths beneath the surface. Solutions that include the solitary wave and periodic traveling waves were considered. The same analysis will be carried out in this present study using BBM approximation.

In the next section of this article, the review of the physical setup of the surface water wave problem is presented, and the derivation of the BBM equation is considered as well. In Section 3, the relations such as equation (2), as well as the expressions for horizontal and vertical velocities at an arbitrary point (x, z) in the fluid is used in connection with exact solutions to examine the particle paths associated to surface solitary waves. Finally, Section 4 highlights the investigation

of particle trajectories in fluid flow beneath periodic surface waves. The essential subject carried out in sections 3 and 4 is the comparison of numerical approximations of the particle paths to the approximate analytical expressions for particle paths.

II. FORMULATION OF THE MATHEMATICAL MODEL FOR THE SURFACE WATER WAVES VIA BOUSSINESQ SCALING

The suppositions of fluid being incompressible and inviscid have been the ground upon which the derivation of the KdV equation is based. Moreover, it is presumed that the flow of the fluid is two-dimensional as well as irrotational and that the function $\eta(x, t)$ could be employed to represent the free surface. Due to these assumptions, the problem at hand may be investigated on the domain $\{(x, z) \in \mathbb{R} \times \mathbb{R} | 0 < z < h_0 + \eta(x, t)\}$ which outstretched to infinity in both positive and negative x -direction, and the parameter h_0 is taken as the undisturbed depth of the fluid [22]. Benjamin, Bona, and Mahoney advocated that the BBM equation modeled the same physical phenomena equally well as the KdV equation, given the same assumptions and approximations that were originally used by Korteweg and de Vries [9]. Based on the given domain, consider the given two-dimensional Euler equations

$$\begin{aligned} u_t + uu_x + vv_z &= -p_x, \\ v_t + uv_x + vv_z &= -p_z - g, \end{aligned}$$

where (u, v) denotes the velocity field, p and g represent the pressure and the acceleration due to gravity, respectively, and suppose the density is taken to be unity. The incompressibility of the fluid together with the irrotationality of the flow are given by

$$u_x + v_z = 0 \quad \text{and} \quad u_z - v_x = 0,$$

respectively. Neglecting the effects of surface tension, the free-surface boundary conditions are given by taking the pressure to equal to atmospheric pressure at the surface and the kinematic boundary condition, as shown below

$$p = p_{atm} \quad \text{and} \quad \eta_t + u\eta_x = v, \quad \text{at } z = h_0 + \eta(x, t). \quad (3)$$

Here, as the fluid is reasoned to be incompressible and irrotational, then we assumed the flow. According to the usual practices, the velocity potential $\phi(x, z, t)$ is introduced. The Laplace equation as a governing equation is used to describes the surface-wave problem, together with the nonlinear boundary conditions (3) on the free surface as well as the regular boundary condition at the bottom.

The establishment of the weakly nonlinear evolution equations of Boussinesq type is attributed to Boussinesq [31] and is comprehensively thrown light on in [21], [19]. The procedure depends on acknowledging the two parameters which express the regime in which waves are known with average wavelength λ , and average amplitude a . The parameter $\alpha = \frac{a}{h_0}$ is used to expresses the relative amplitude of the waves, while the parameter $\beta = \frac{h_0^2}{\lambda^2}$ estimates the 'shallowness' of the fluid in connection to the wavelength. It has been shown in [19] that to second-order accuracy in α and β , the solutions to the free-surface problem discussed

above may be accurately estimated by solutions of the system given by

$$\begin{aligned} \eta_t + h_0 w_x + (\eta w)_x + \frac{1}{6} h_0^3 \eta_{xxt} &= 0, \\ w_t + g \eta_x + w w_x - \frac{1}{2} h_0^2 w_{xxt} &= 0, \end{aligned}$$

where η represents the excursion of the free surface, w represents the horizontal velocity at the bottom of the medium.

From the notion of fluid being incompressible, the potential function ϕ satisfies the Laplace's equation in the domain specified above. The problem together with the necessary conditions is given by [32].

$$\begin{aligned} \phi_{xx} + \phi_{zz} &= 0 \quad \text{in } -h_0 < z < \eta(x, t), \\ \phi_z &= 0 \quad \text{in } z = -h_0, \end{aligned} \tag{4}$$

with the surface boundary conditions

$$\left. \begin{aligned} \eta_t + \phi_x \eta_x - \phi_z &= 0, \\ \phi_t + \frac{1}{2} (\phi_x^2 + \phi_z^2) + g \eta &= 0, \end{aligned} \right\} \text{ on } z = \eta(x, t). \tag{5}$$

Next, we derived the system of BBM equation and other equations needed in this article for the interested reader. The background of this study is traced back to Whitham and Bona et al., [21], [19]. Derivation of the BBM equation required the assumption of fluid being incompressible and inviscid in a constant gravitational field as well as assuming small-amplitude shallow water. Let the vertical surface be denoted as $z = \eta + h_0$, where z represents the distance measured from the horizontal bottom.

The shallow water theory, with ϕ_x approximately independent of z , and the small total depth both suggest an expansion

$$\phi = \sum_{n=0}^{\infty} z^n f_n(x, t).$$

When this is substituted into Laplace's equation (4), and the boundary condition $\phi_z = 0$ on $z = 0$ is used, we get

$$\phi = \sum_{m=0}^{\infty} (-1)^m \frac{z^{2m}}{(2m)!} \frac{\partial^{2m} f}{\partial x^{2m}}, \tag{6}$$

where $f = f_0$. For the convenience, normalizing the variables from the start will be a good idea by using

$$x = lx', \quad z = h_0 z', \quad t = \frac{lt'}{c_0}, \quad \eta = a \eta', \quad \psi = \frac{gl a \psi'}{c_0},$$

where a is the amplitude and $c_0 = \sqrt{gh_0}$ represents the phase velocity. The primed variables are normalized, while the ones without prime are original variables. In normalized form Laplace's equation together with boundary condition (4) yields:

$$\phi = \sum_{m=0}^{\infty} (-1)^m \frac{z'^{2m}}{(2m)!} \frac{\partial^{2m} f}{\partial x'^{2m}} \beta^m = f - \frac{z'^2}{2} f_{x'x'} \beta + \mathcal{O}(\beta^2), \tag{7}$$

substituting equation (7) into the boundary conditions at the

free surface resulting in

$$\begin{aligned} \eta'_t + \{(1 + \alpha \eta') f_{x'}\}_{x'} - \left\{ \frac{1}{6} (1 + \alpha \eta')^3 f_{x'x'x'} \right. \\ \left. + \frac{1}{2} \alpha (1 + \alpha \eta')^2 \eta'_{x'} f_{x'x'} \right\} \beta + \mathcal{O}(\beta^2) &= 0, \end{aligned} \tag{8}$$

$$\begin{aligned} \eta' + f_{t'} + \frac{1}{2} \alpha f_{x'}^2 - \frac{1}{2} (1 + \alpha \eta')^2 \left\{ f_{x'x't'} \right. \\ \left. + \alpha f_{x'} f_{x'x't'} - \alpha f_{x'}^2 \right\} \beta + \mathcal{O}(\beta^2) &= 0. \end{aligned} \tag{9}$$

If the terms in the first power of β are retained, but the term of $\mathcal{O}(\alpha\beta)$ are dropped and differentiating equation (9) for x' , the variants of Boussinesq's system is obtained as

$$\eta'_{t'} + w_{x'} + \alpha (\eta' w)_{x'} - \frac{1}{6} \beta w_{x'x'x'} + \mathcal{O}(\alpha\beta, \beta^2) = 0, \tag{10}$$

$$\begin{aligned} w_{t'} + \eta'_{x'} + \alpha w w_{x'} - \frac{1}{2} \beta w_{x't't'} + \mathcal{O}(\alpha\beta, \beta^2) &= 0, \\ w &= f_{x'}. \end{aligned} \tag{11}$$

Differentiating equation (7) with respect to x' , the horizontal velocity is expressed as

$$u(x, z, t) = \phi_{x'} = w - \frac{z'^2}{2} w_{x'x'} \beta + \mathcal{O}(\beta^2). \tag{12}$$

Similarly, the vertical velocity can be written as

$$v(x, z, t) = \phi_{z'} = -z' w_{x'} \beta + \mathcal{O}(\beta^2). \tag{13}$$

The KdV equation can be derived from any of the systems in equations (10) and (11) by concentrating on the wave moving to the right only. If the terms of order α and β are neglected from equations (10) and (11), the solution gives

$$w = \eta', \quad \eta'_{t'} + \eta'_{x'} = 0.$$

Taking some assumptions and simplifications into consideration, we arrive at the expressions

$$w = \eta' - \frac{1}{4} \alpha \eta'^2 + \frac{1}{3} \beta \eta'_{x'x'} + \mathcal{O}(\alpha^2 + \beta^2), \tag{14}$$

$$\eta'_{t'} + \eta'_{x'} + \frac{3}{2} \alpha \eta' \eta'_{x'} + \frac{1}{6} \beta \eta'_{x'x'x'} + \mathcal{O}(\alpha^2 + \beta^2) = 0. \tag{15}$$

The relation (14) is similar to Riemann invariant and equation (15) is the normalized form of KdV equation.

Using the parameters defined earlier, the normalized variables is changed into the original variables, α and β , were also dropped so that we arrive at

$$w = \eta - \frac{1}{4} \eta^2 + \frac{1}{3} \eta_{xx}, \tag{16}$$

and the KdV equation in the form [22]

$$\eta_t + c_0 \eta_x + \frac{3}{2} \frac{c_0}{h_0} \eta \eta_x + \frac{1}{6} c_0 h_0^2 \eta_{xxx} = 0. \tag{17}$$

Then, using the KdV equation in (17), the BBM equation is derived by neglecting nonlinear and higher order terms so that we are left with $\eta_x = -\frac{1}{c_0} \eta_t$. Using this in the last term of equation (17) yields

$$\eta_t + c_0 \eta_x + \frac{3}{2} \frac{c_0}{h_0} \eta \eta_x - \frac{1}{6} h_0^2 \eta_{xxt} = 0. \tag{18}$$

Equation (18) is the BBM model considered in this study. It is given in non-dimensional form as

$$\eta_t + \eta_x + \frac{3}{2}\eta\eta_x - \frac{1}{6}\eta_{xxt} = 0.$$

Finally, we have the system

$$w = \eta - \frac{1}{4}\eta^2 + \frac{1}{3}\eta_{xx}, \tag{19}$$

$$\eta_t + \eta_x + \frac{3}{2}\eta\eta_x - \frac{1}{6}\eta_{xxt} = 0. \tag{20}$$

Dropping the prime and β in equations (12) and (13), the expression for the horizontal velocity of the fluid particle is given in non-dimensional variable as

$$u(x, z, t) = w - \frac{z^2}{2}w_{xx}, \tag{21}$$

which is improved to read

$$u(x, z, t) = \eta - \frac{1}{4}\eta^2 + \left(\frac{1}{3} - \frac{z^2}{2}\right)\eta_{xx}. \tag{22}$$

Similarly, the vertical velocity is given as

$$v(x, z, t) = -zw_x. \tag{23}$$

III. PARTICLE TRAJECTORIES IN SOLITARY-WAVE SOLUTIONS

Our focus will be centered on the particle trajectories in the fluid because of the passage of a solitary wave at the surface. The exact solution of the BBM equation in regards to solitary-wave is given by

$$\eta(x, t) = \eta_0 \operatorname{sech}^2\left(\frac{1}{2}\sqrt{\frac{6\eta_0}{2+\eta_0}}(x-x_0-ct)\right), \tag{24}$$

where η_0 represents the amplitude, x_0 denotes the initial point of the wave crest, and the phase velocity c is given by

$$c = 1 + \frac{\eta_0}{2}. \tag{25}$$

Assuming that the wave crest is positioned at $x = 0$ at time $t = 0$, so that $x_0 = 0$, then the solitary-wave solution of the BBM equation given in (24) becomes

$$\eta(x, t) = \eta_0 \operatorname{sech}^2\left(\frac{1}{2}\sqrt{\frac{6\eta_0}{2+\eta_0}}(x-ct)\right). \tag{26}$$

Let the argument $\mathcal{A} = \frac{1}{2}\sqrt{\frac{6\eta_0}{2+\eta_0}}(x-ct)$ be defined. Substituting the solitary-wave solution of the BBM equation given in (26) into the relation (19), then we got the expression

$$w = \eta_0 \operatorname{sech}^2(\mathcal{A}) \left\{ 1 - \frac{\eta_0}{4} \operatorname{sech}^2(\mathcal{A}) - \frac{\eta_0}{2+\eta_0} [3\operatorname{sech}^2(\mathcal{A}) - 2] \right\}, \tag{27}$$

for the horizontal velocity. The derivative of the horizontal velocity computed above is given by

$$w_x = \frac{\eta_0}{2} \sqrt{\frac{6\eta_0}{2+\eta_0}} \operatorname{sech}^2(\mathcal{A}) \tanh(\mathcal{A}) \left\{ -2 + \eta_0 \operatorname{sech}^2(\mathcal{A}) + \frac{4\eta_0}{2+\eta_0} (3\operatorname{sech}^2(\mathcal{A}) - 1) \right\}. \tag{28}$$

Using equations (22) and (23) in connection to the relations (26) and (28), the velocity components, that is, the horizontal and vertical velocities at an arbitrary point (x, z) in the fluid, and at a given time t are computed as

$$u(x, z, t) = \eta_0 \operatorname{sech}^2(\mathcal{A}) \left\{ 1 - \frac{\eta_0}{4} \operatorname{sech}^2(\mathcal{A}) - \frac{3\eta_0}{2+\eta_0} \left(\frac{1}{3} - \frac{z^2}{2}\right) [3\operatorname{sech}^2(\mathcal{A}) - 2] \right\}, \tag{29}$$

$$v(x, z, t) = -z \frac{\eta_0}{2} \sqrt{\frac{6\eta_0}{2+\eta_0}} \operatorname{sech}^2(\mathcal{A}) \tanh(\mathcal{A}) \left\{ -2 + \eta_0 \operatorname{sech}^2(\mathcal{A}) + \frac{4\eta_0}{2+\eta_0} (3\operatorname{sech}^2(\mathcal{A}) - 1) \right\}. \tag{30}$$

Let the functions $\xi(t)$ and $\zeta(t)$ denote the x -coordinate and z -coordinate, respectively, of a particle initially positioned at the point $(x, z) = (\xi_0, \zeta_0)$. Then, the particle movement is given by the differential equations

$$\frac{\partial \xi}{\partial t} = u(\xi(t), \zeta(t), t), \quad \frac{\partial \zeta}{\partial t} = v(\xi(t), \zeta(t), t), \tag{31}$$

with the initial conditions $\xi(0) = \xi_0$ and $\zeta(0) = \zeta_0$. The solutions to these equations can be obtained numerically. For example, the fourth-order Runge-Kutta method can be efficiently implemented for the discretization of the given equations. It has been verified that such a method produces highly accurate results based on numerical experimental results even when a small-time step is used.

In addition, for comparison purposes, a closed-form solution that illustrates approximate particle trajectories will be computed and see its deviation from the numerical approximation. If we assumed that during the process of moving of a solitary wave, each particle do not move in a large amount, then the equations (31) can be approximated by

$$\frac{\partial \bar{\xi}}{\partial t} = u(\xi_0, \zeta_0, t), \quad \frac{\partial \bar{\zeta}}{\partial t} = v(\xi_0, \zeta_0, t), \tag{32}$$

where the initial condition is still the same as (ξ_0, ζ_0) . Hence, using equation (32) and the solutions of BBM equation given in equations (24) and (27) we find the expressions

$$\bar{\xi} = X_0 - \frac{2\eta_0}{c} \sqrt{\frac{2+\eta_0}{6\eta_0}} \tanh(\mathcal{A}_0) \left\{ 1 - \frac{\eta_0}{6} - \frac{\eta_0}{12} \operatorname{sech}^2(\mathcal{A}_0) - \frac{3\eta_0}{2+\eta_0} \left(\frac{1}{3} - \frac{\zeta_0^2}{2}\right) \operatorname{sech}^2(\mathcal{A}_0) \right\}, \tag{33}$$

$$\bar{\zeta} = Z_0 + \frac{\zeta_0}{c} \eta_0 \operatorname{sech}^2(\mathcal{A}_0) \left\{ 1 - \frac{\eta_0}{4} \operatorname{sech}^2(\mathcal{A}_0) - \frac{\eta_0}{2+\eta_0} [3\operatorname{sech}^2(\mathcal{A}_0) - 2] \right\}. \tag{34}$$

Here \mathcal{A}_0 denotes the argument $\mathcal{A}_0(t) = \frac{1}{2}\sqrt{\frac{6\eta_0}{2+\eta_0}}(\xi_0-ct)$ which corresponds to a solitary wave which is originally located at $x = 0$, and a particle whose x -coordinate is first given as $x = \xi_0$. The constants X_0 and Z_0 represent the difference between the initial particle position ξ_0 and

ζ_0 respectively after the integration, and the expressions on the right-hand sides are computed at $t = 0$ (i.e. at $\mathcal{A}_0(0) = \frac{1}{2} \sqrt{\frac{6\eta_0}{2 + \eta_0}}(\xi_0)$) in both cases.

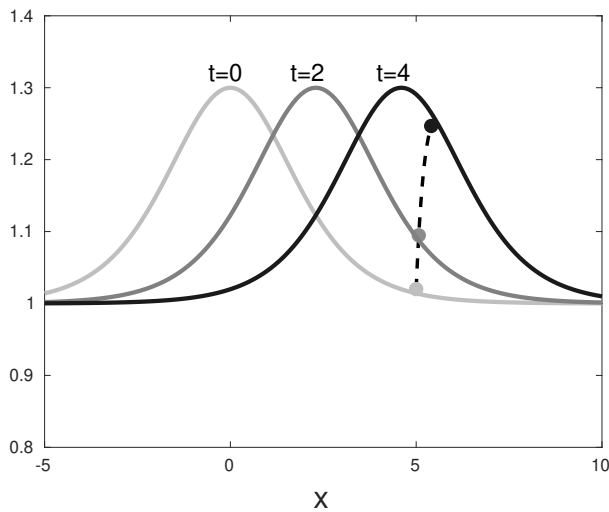


Fig. 1: The wave profile is shown at $t = 0$ (light-gray), $t = 2$ (dark-gray) and $t = 4$ (black) as indicated in the figure. The particle trajectory originally located on the surface at $(5, 1.02)$ is denoted by the dashed curve. The particle lagging behind the surface reveals that the expression used in equations (33) and (34) yields a small error.

The surface profile and the particle trajectories throughout the propagation of the solitary wave with amplitude $\eta_0 = 0.3$ are shown in figures 1–3. The y -coordinate indicates the values of z in every figure included in this paper unless specified otherwise. Figure 1 reveals the time evolution of the fluid particle at the surface of the fluid, and the wave profile is displayed at $t = 0$ (light-gray), $t = 2$ (dark-gray) and $t = 4$ (black). The dashed curve described the particle path provided by approximations (33) and (34). Different color is used to denote the position of the particle on the wave profile; the light-gray spot shows the particle location at time $t = 0$, while the dark-gray spot and the black spot show the particle position at time $t = 4$ and $t = 6$ respectively. Moreover, the same color indication is used in Figures 2 and 3. It worth noting from these figures that if the fluid particles are positioned to the right side of the crest, then they tend to go towards the right and upwards as shown in figure 1, while the fluid particles go towards the right and downwards if they are positioned to the left of the crest as illustrated in figure 2. This concurred with the discoveries of Borluk and Kalisch [22] and Constantin and Escher [23]. Figure 3 demonstrates the particle trajectories during one complete wave cycle. It is evident that the particles which are closer to the bed produce a smaller total excursion. It is regarded that the vertical excursion is smaller when compared to its horizontal displacement and decreases quickly with the depth of the trajectory beneath the free surface. Hence, the particles near the bottom possess a smaller amplitude and the path becomes more or less a straight line at the bottom since the vertical motion of the particle is zero, and just a horizontal displacement remains in existence. These results are in agreement with the results obtained by Khorsand [33] as well as Borluk and Kalisch [22].

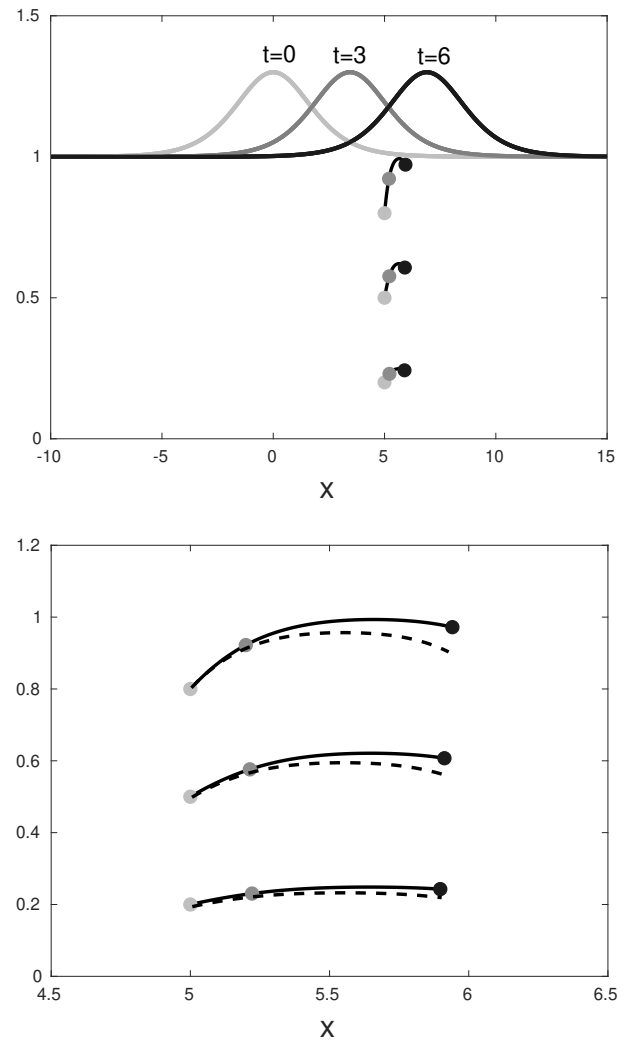


Fig. 2: The wave in the upper panel is shown at $t = 0$ (light-gray), $t = 3$ (dark-gray) and $t = 6$ (black). As in Figure 1, the wave crest is initially located at $x = 0$. The paths of the fluid particles shown were initially located at $(5, 0.8)$, $(5, 0.5)$ and $(5, 0.2)$. A different color is used to denote the particle locations as shown in the three different cases presented. The light-gray dots describe the particle locations at time $t = 0$. The dark-gray dots describe the particle locations at time $t = 3$. The black dots describe the particle locations at time $t = 6$. In the lower panel, the particle paths computed using the RungeKutta method (solid) are compared to the approximate relations (33) and (34) (dashed).

In the upper panels of Figures 2 and 3, the particle paths shown as the solid curves represent the numerical solutions of relations (29) and (30) which is obtained by the fourth-order Runge-Kutta method. The comparison of the numerical solutions of particle paths obtained using the expressions given in (31) and the approximate analytic solutions in equations (33) and (34) indicated as dashed curves are shown in the lower panels of Figures 2 and 3. We see from these two comparisons that the particle trajectories produced by the approximations (33) and (34) are slightly shorter than the more accurate paths computed numerically.

Using equation (34), the maximal ride of a particle from rest into the vertical path can be evaluated by taking $\xi_0 = 0$ from the argument $\mathcal{A}_0(t) = \frac{1}{2} \sqrt{\frac{6\eta_0}{2 + \eta_0}}(\xi_0 - ct)$ which

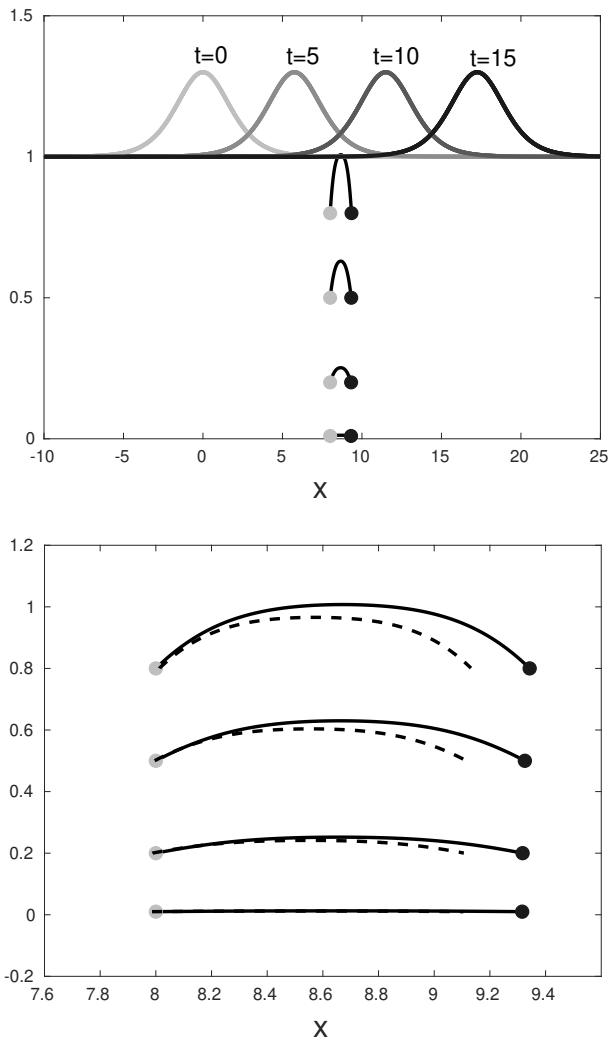


Fig. 3: The wave profile in the upper panel is shown at $t = 0, t = 5, t = 10$ and $t = 15$. The paths of the fluid particles shown were initially located at $(8, 0.8), (8, 0.5), (8, 0.2), (8, 0.01)$. The light-gray dots describe the particle positions at time $t = 0$, and the black dots describe the particle positions at time $t = 6$. The curves indicate the paths traced out by particles during the transition from the left to the right. In the lower panel, a comparison of the particle paths obtained numerically (solid) and analytically by relations (33) and (34) (dashed) is shown.

corresponds to a solitary wave, then we have

$$\mathcal{A}_0(t) = -\frac{1}{2} \sqrt{\frac{6\eta_0}{2 + \eta_0}} ct, \tag{35}$$

using equation (35), $\mathcal{A}_0 = 0$ when $t = 0$, and $\mathcal{A}_0 = \infty$ when $t = -\infty$. We have seen that $\mathcal{A}_0 = 0$ when $\xi_0 = 0$ and $t = 0$. So therefore, using these in relation (34), the simplification yields

$$\bar{\zeta}(t = 0) = Z_0 + \frac{\zeta_0}{c} \eta_0 \left\{ 1 - \frac{\eta_0}{4} - \frac{\eta_0}{2 + \eta_0} \right\}. \tag{36}$$

Again, when $\xi_0 = 0$ and $t = -\infty$, we have $\mathcal{A}_0 = \infty$. Applying these into equation (34) yields

$$\bar{\zeta}(t = -\infty) = Z_0. \tag{37}$$

Subtracting equation (37) from equation (36) gives,

$$\bar{\zeta}(t = 0) - \bar{\zeta}(t = -\infty) = \frac{\zeta_0}{c} \eta_0 \left\{ 1 - \frac{\eta_0}{4} - \frac{\eta_0}{2 + \eta_0} \right\}.$$

Since $c = 1 + \frac{\eta_0}{2}$, then the above equation becomes

$$\bar{\zeta}(t = 0) - \bar{\zeta}(t = -\infty) = \zeta_0 \frac{2\eta_0}{2 + \eta_0} \left\{ 1 - \frac{\eta_0}{4} - \frac{\eta_0}{2 + \eta_0} \right\}, \tag{38}$$

where ζ_0 represents the initial z -coordinate of the particle. The decline attitude exhibited in the total vertical excursion with the increasing depths, which was seen in Figure 3, is as a result of this expression. As particle amplitudes decompose exponentially in the bottom direction in the case of linear waves, such behavior is expected.

Next, relation (33) is considered. Setting $\xi_0 = 0$ and $t = \infty$, then $\mathcal{A}_0 = -\infty$, using these in relation (33) yields an expression

$$\bar{\xi}(t = \infty) = X_0 + \frac{2\eta_0}{c} \sqrt{\frac{2 + \eta_0}{6\eta_0}} \left\{ 1 - \frac{\eta_0}{6} \right\}. \tag{39}$$

Again, setting $\xi_0 = 0$ and $t = -\infty$, we have $\mathcal{A}_0 = \infty$, so relation (33) yields

$$\bar{\xi}(t = -\infty) = X_0 - \frac{2\eta_0}{c} \sqrt{\frac{2 + \eta_0}{6\eta_0}} \left\{ 1 - \frac{\eta_0}{6} \right\}. \tag{40}$$

Subtracting equation (40) from equation (39) produces

$$\bar{\xi}(t = \infty) - \bar{\xi}(t = -\infty) = \frac{4\eta_0}{c} \sqrt{\frac{2 + \eta_0}{6\eta_0}} \left\{ 1 - \frac{\eta_0}{6} \right\}.$$

Therefore, the mass flux due to the passage of a solitary wave is evaluated from (33) and yields the expression

$$\bar{\xi}(t = \infty) - \bar{\xi}(t = -\infty) = 4\eta_0 \sqrt{\frac{2 + \eta_0}{6\eta_0}} \frac{\left\{ 1 - \frac{\eta_0}{6} \right\}}{\left\{ 1 + \frac{\eta_0}{2} \right\}}. \tag{41}$$

Since the nondimensional depth of the fluid is 1, this expression denotes the total mass flux in a vertical cross-section in the fluid owing to the motion of a solitary wave. Since the BBM equation under consideration is

$$\eta_t + \eta_x + \frac{3}{2} \eta \eta_x - \frac{1}{6} \eta_{xxt} = 0.$$

According to Ali and Kalisch [34], this implies

$$\frac{\partial}{\partial t} (h_0 + \eta) + \frac{\partial}{\partial x} \left(\eta + \frac{3}{4} \eta^2 - \frac{1}{6} \eta_{xt} \right) = 0. \tag{42}$$

Also, the mass flux due to the motion of a solitary wave can be evaluated by noting that the BBM equation (1) is an approximate mass conservation equation. The quantity

$$q_M = \eta + \frac{3}{4} \eta^2 - \frac{1}{6} \eta_{xt}, \tag{43}$$

can be expressed accordingly as the mass flux due to the wave motion. In [34], the expression $q_M = \eta + \frac{3}{4} \eta^2 + \frac{1}{6} \eta_{xt}$, was found, but these are equivalent to within the order of approximation. Hence, the total mass flux can be evaluated from the integral

$$Q = \int_{-\infty}^{\infty} q_M dt. \tag{44}$$

Note that

$$\begin{aligned} \mathcal{A} &= \frac{1}{2} \sqrt{\frac{6\eta_0}{2 + \eta_0}} (x - ct) \Rightarrow \frac{d\mathcal{A}}{dt} = -\frac{c}{2} \sqrt{\frac{6\eta_0}{2 + \eta_0}} \\ &\Rightarrow dt = -\frac{2}{c} \sqrt{\frac{2 + \eta_0}{6\eta_0}} d\mathcal{A}. \end{aligned} \tag{45}$$

However, transformation of the integral's limit and substitution of equations (45) and (43) into equation (44) yields

$$Q = \frac{2}{c} \sqrt{\frac{2 + \eta_0}{6\eta_0}} \int_{-\infty}^{\infty} \left(\eta + \frac{3}{4}\eta^2 - \frac{1}{6}\eta_{xt} \right) dA.$$

Here η_{xt} is neglected because it is integrated to zero, so

$$Q = \frac{2}{c} \sqrt{\frac{2 + \eta_0}{6\eta_0}} \int_{-\infty}^{\infty} \left(\eta + \frac{3}{4}\eta^2 \right) dA.$$

Substituting expressions of η and η^2 into the above equation gives

$$Q = \frac{2}{c} \sqrt{\frac{2 + \eta_0}{6\eta_0}} \int_{-\infty}^{\infty} \left\{ \eta_0 \operatorname{sech}^2(A) + \frac{3}{4}\eta_0^2 \operatorname{sech}^4(A) \right\} dA,$$

integration gives

$$Q = \frac{2\eta_0}{c} \sqrt{\frac{2 + \eta_0}{6\eta_0}} \left\{ \tanh(A) + \frac{\eta_0}{4} [3 \tanh(A) - \tanh^3(A)] \right\}_{-\infty}^{\infty}.$$

Therefore, this yields

$$Q = 4\eta_0 \sqrt{\frac{2 + \eta_0}{6\eta_0}}.$$

Comparing the value gotten here to the expression found in equation (41), we have

$$\begin{aligned} 4\eta_0 \sqrt{\frac{2 + \eta_0}{6\eta_0}} - 4\eta_0 \sqrt{\frac{2 + \eta_0}{6\eta_0}} \left\{ \frac{1 - \frac{\eta_0}{6}}{1 + \frac{\eta_0}{2}} \right\} \\ = \frac{8\eta_0^{3/2}}{3} \sqrt{\frac{2 + \eta_0}{6}} + \mathcal{O}(\eta_0^{5/2}). \end{aligned}$$

Here, it is observed that the mass flux evaluated from the relation (43) is larger by a moderate amount, and the difference between them is less than order two as shown in the computation above. The further evaluation of relations (32) has led to the establishment of the formula for the mass flux which was directly found from the particle trajectories above, and it is shown that the horizontal displacement of a particle was underestimated by making a comparison with the Runge-Kutta method.

In Figure 4, it is shown that the value of mass flux evaluated using the Runge-Kutta method is very close to the value of $Q = 4\eta_0 \sqrt{\frac{2 + \eta_0}{6\eta_0}}$, and much more accurate than the value gotten when relation (41) is used.

IV. PARTICLE TRAJECTORIES IN PERIODIC WAVES

Our focus will now be on particle trajectories in the fluid flow due to the transmission of periodic traveling waves at the surface. In [35], the periodic wavetrains of KdV approximation are defined by exact solutions of which are expressed as cnoidal functions. The same concept is used here for BBM approximation. The periodic solutions of BBM equation (1) are given by

$$\eta = f_2 + (f_1 - f_2) \operatorname{cn}^2(\mathcal{B}), \quad (46)$$

where the constants f_1 , f_2 and f_3 which are given in the order $f_3 < f_2 < f_1$ are used to described the solution.

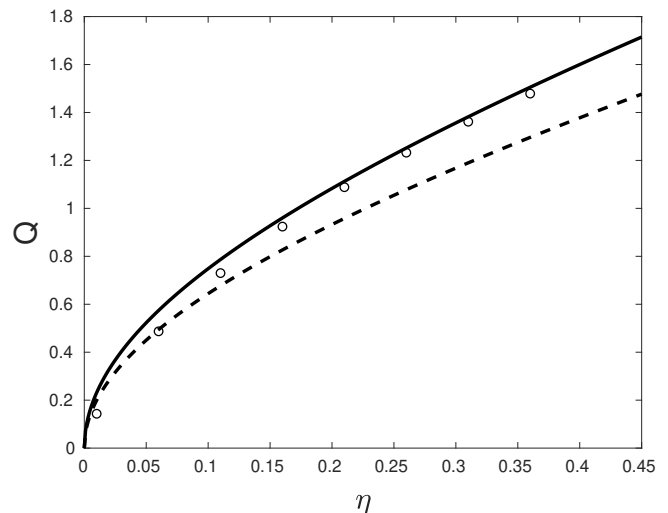


Fig. 4: The values of total mass flux are compared in this figure. The dashed line describes the value computed in relation (41), while the solid line describes the formula $4\eta_0 \sqrt{\frac{2 + \eta_0}{6\eta_0}}$. The mass flux evaluated from the numerical solution of the solitary-wave particle paths using the Runge-Kutta method is described by the circles. Here, note that the average over the depth of the fluid was taken.

The argument of equation (46) is given by $\mathcal{B}(x, t) = \frac{1}{2} \sqrt{\frac{6}{2 + (f_1 - f_3)}} (f_1 - f_3)^{1/2} (x - ct)$, cn is one of the Jacobian elliptic functions defined by the incomplete elliptic integral of the first kind [22], [36], and the modulus m of this Jacobian elliptic function is given by $m = \frac{f_1 - f_2}{f_1 - f_3}$. The phase speed and the wavelength of the wave are given by $c = 1 + \frac{(f_1 + f_2 + f_3)}{2}$ and $\lambda = 4 \sqrt{\frac{2 + (f_1 - f_3)}{6}} K(m) \frac{1}{\sqrt{f_1 - f_3}}$ respectively, where $K(m)$ is the complete elliptic integral of the first kind.

The particle motion which is described by equation (31) will be used in conjunction with equations (21) and (23), which implies

$$\frac{\partial \xi}{\partial t} = w - \frac{\zeta^2}{2} w_{xx}, \quad (47)$$

$$\frac{\partial \zeta}{\partial t} = -\zeta w_x. \quad (48)$$

The derivatives of the relation (46) are given by

$$\eta_x = -\sqrt{\frac{6}{2 + (f_1 - f_3)}} (f_1 - f_2) (f_1 - f_3)^{1/2} \operatorname{cn}(\mathcal{B}) \operatorname{sn}(\mathcal{B}) \operatorname{dn}(\mathcal{B}), \quad (49)$$

$$\begin{aligned} \eta_{xx} = & \frac{3}{2 + (f_1 - f_3)} (f_1 - f_2) (f_1 - f_3) \operatorname{sn}^2(\mathcal{B}) \operatorname{dn}^2(\mathcal{B}) \\ & - \frac{3}{2 + (f_1 - f_3)} (f_1 - f_2) (f_1 - f_3) \operatorname{cn}^2(\mathcal{B}) \operatorname{dn}^2(\mathcal{B}) \\ & + \frac{3}{2 + (f_1 - f_3)} m (f_1 - f_2) (f_1 - f_3) \operatorname{sn}^2(\mathcal{B}) \operatorname{cn}^2(\mathcal{B}). \end{aligned} \quad (50)$$

Upon substitution into relation (19), the horizontal velocity in terms of the Jacobian elliptic functions is given as

$$w = f_2 - \frac{1}{4}f_2^2 + (f_1 - f_2) \left(1 - \frac{f_2}{2}\right) \text{cn}^2(\mathcal{B}) - \frac{1}{4}(f_1 - f_2)^2 \text{cn}^4(\mathcal{B}) - \frac{1}{2 + (f_1 - f_3)}(f_1 - f_2)(f_1 - f_3) \times \left\{ -\text{sn}^2(\mathcal{B})\text{dn}^2(\mathcal{B}) + \text{cn}^2(\mathcal{B})\text{dn}^2(\mathcal{B}) - m \text{sn}^2(\mathcal{B})\text{cn}^2(\mathcal{B}) \right\}.$$

The derivatives of this horizontal velocity are given by

$$w_x = \frac{1}{2} \sqrt{\frac{6}{2 + (f_1 - f_3)}} (f_1 - f_3)^{1/2} \text{sn}(\mathcal{B})\text{cn}(\mathcal{B})\text{dn}(\mathcal{B}) \times \left\{ - (f_1 - f_2)(2 - f_2) + (f_1 - f_2)^2 \text{cn}^2(\mathcal{B}) + \frac{4}{2 + (f_1 - f_3)}(f_1 - f_2)(f_1 - f_3)(\text{dn}^2(\mathcal{B}) + m \text{cn}^2(\mathcal{B}) - m \text{sn}^2(\mathcal{B})) \right\}, \quad (51)$$

and

$$w_{xx} = \frac{1}{2} \cdot \frac{3}{2 + (f_1 - f_3)} (f_1 - f_3) \left\{ - (f_1 - f_2)(2 - f_2) \times (\text{cn}^2(\mathcal{B})\text{dn}^2(\mathcal{B}) - \text{sn}^2(\mathcal{B})\text{dn}^2(\mathcal{B}) - m \text{sn}^2(\mathcal{B})\text{cn}^2(\mathcal{B})) + (f_1 - f_2)^2 (\text{cn}^4(\mathcal{B})\text{dn}^2(\mathcal{B}) - 3\text{sn}^2(\mathcal{B})\text{cn}^2(\mathcal{B})\text{dn}^2(\mathcal{B}) - m \text{sn}^2(\mathcal{B})\text{cn}^4(\mathcal{B})) + \left(\frac{4}{2 + (f_1 - f_3)}(f_1 - f_2)(f_1 - f_3)\right) \times [(\text{cn}^2(\mathcal{B})\text{dn}^2(\mathcal{B}) - \text{sn}^2(\mathcal{B})\text{dn}^2(\mathcal{B}) - m \text{sn}^2(\mathcal{B})\text{cn}^2(\mathcal{B}))][\text{dn}^2(\mathcal{B}) + m \text{cn}^2(\mathcal{B}) - m \text{sn}^2(\mathcal{B})] - 6m \text{sn}^2(\mathcal{B})\text{cn}^2(\mathcal{B})\text{dn}^2(\mathcal{B}) \right\}.$$

Hence, for the periodic-wave solutions of the BBM equation, the horizontal and vertical velocities at an arbitrary point (x, z) in the fluid, and at a time t are computed as

$$u(x, z, t) = f_2 - \frac{1}{4}f_2^2 + (f_1 - f_2) \left(1 - \frac{f_2}{2}\right) \text{cn}^2(\mathcal{B}) - \frac{1}{4}(f_1 - f_2)^2 \text{cn}^4(\mathcal{B}) - \frac{1}{2 + (f_1 - f_3)}(f_1 - f_2)(f_1 - f_3) \times \left\{ -\text{sn}^2(\mathcal{B})\text{dn}^2(\mathcal{B}) + \text{cn}^2(\mathcal{B})\text{dn}^2(\mathcal{B}) - m \text{sn}^2(\mathcal{B})\text{cn}^2(\mathcal{B}) \right\} - \frac{\zeta^2}{4} \cdot \frac{3}{2 + (f_1 - f_3)} (f_1 - f_3) \left\{ - (f_1 - f_2)(2 - f_2) \times (\text{cn}^2(\mathcal{B})\text{dn}^2(\mathcal{B}) - \text{sn}^2(\mathcal{B})\text{dn}^2(\mathcal{B}) - m \text{sn}^2(\mathcal{B})\text{cn}^2(\mathcal{B})) + (f_1 - f_2)^2 (\text{cn}^4(\mathcal{B})\text{dn}^2(\mathcal{B}) - 3\text{sn}^2(\mathcal{B})\text{cn}^2(\mathcal{B})\text{dn}^2(\mathcal{B}) - m \text{sn}^2(\mathcal{B})\text{cn}^4(\mathcal{B})) + \left(\frac{4}{2 + (f_1 - f_3)}(f_1 - f_2)(f_1 - f_3)\right) \times [(\text{cn}^2(\mathcal{B})\text{dn}^2(\mathcal{B}) - \text{sn}^2(\mathcal{B})\text{dn}^2(\mathcal{B}) - m \text{sn}^2(\mathcal{B})\text{cn}^2(\mathcal{B}))][\text{dn}^2(\mathcal{B}) + m \text{cn}^2(\mathcal{B}) - m \text{sn}^2(\mathcal{B})] - 6m \text{sn}^2(\mathcal{B})\text{cn}^2(\mathcal{B})\text{dn}^2(\mathcal{B}) \right\}, \quad (52)$$

$$v(x, z, t) = -\frac{\zeta}{2} \sqrt{\frac{6}{2 + (f_1 - f_3)}} (f_1 - f_3)^{1/2} \text{sn}(\mathcal{B})\text{cn}(\mathcal{B})\text{dn}(\mathcal{B}) \times \left\{ - (f_1 - f_2)(2 - f_2) + (f_1 - f_2)^2 \text{cn}^2(\mathcal{B}) + \frac{4}{2 + (f_1 - f_3)}(f_1 - f_2)(f_1 - f_3)(\text{dn}^2(\mathcal{B}) + m \text{cn}^2(\mathcal{B}) - m \text{sn}^2(\mathcal{B})) \right\}. \quad (53)$$

After this computation, the equations (47) and (48) may be integrated numerically provided the initial particle position (ξ_0, ζ_0) is known. For comparison, the approximate particle trajectories of the periodic waves in a closed-form will be computed as we did in the case of solitary-wave solutions. However, the relation (32) is used to define the particle trajectories in the periodic waves since the fluid particles may not be reposition considerably from their initial location during the transition of a surface wave. At this point, relations (47) and (48) is used with the right-hand side fixed at the initial particle location. Afterward using the expression (19), the x -component of the particle trajectory is found to be

$$\int \partial \bar{\xi} = \int_0^t \left\{ w - \frac{\zeta_0^2}{2} w_{xx} \right\} dt',$$

which can also be written as

$$\bar{\xi} - \xi_0 = \int_0^t \left\{ w - \frac{\zeta_0^2}{2} w_{xx} \right\} dt',$$

then

$$\bar{\xi} - \xi_0 = \int_0^t \left\{ \eta - \frac{1}{4}\eta^2 + \frac{1}{3}\eta_{xx} \right\} dt' - \frac{\zeta_0^2}{2} \int_0^t w_{xx} dt',$$

where the integrands are evaluated at (ξ_0, t') , then the x -derivatives can be written in terms of t derivatives, so that

$$\bar{\xi} - \xi_0 = \int_0^t \left\{ \eta - \frac{1}{4}\eta^2 \right\} dt' + \left\{ -\frac{1}{3c}\eta_x + \frac{\zeta_0^2}{2c}w_x \right\}_0^t. \quad (54)$$

We define $\mathcal{B}_0(t) = \frac{1}{2} \sqrt{\frac{6}{2 + (f_1 - f_3)}} (f_1 - f_3)^{1/2} (\xi_0 - ct)$, and the first term of (54) is integrated to

$$\int_0^t \left\{ \eta - \frac{1}{4}\eta^2 \right\} dt' = \left(f_2 - \frac{f_2^2}{4}\right) t - \frac{(f_1 - f_2)}{c(f_1 - f_3)^{1/2}} \sqrt{\frac{2 + (f_1 - f_3)}{6}} (2 - f_2) \int_{\mathcal{B}_0(0)}^{\mathcal{B}_0(t)} \text{cn}^2(\mathcal{B}) d\mathcal{B} + \frac{(f_1 - f_2)^2}{2c(f_1 - f_3)^{1/2}} \sqrt{\frac{2 + (f_1 - f_3)}{6}} \int_{\mathcal{B}_0(0)}^{\mathcal{B}_0(t)} \text{cn}^4(\mathcal{B}) d\mathcal{B}.$$

The last two integrals are given by

$$\int \text{cn}^2(\mathcal{B}) d\mathcal{B} = \mathcal{B} - \frac{\mathcal{B}}{m} + \frac{E(\text{am}(\mathcal{B}), m)}{m},$$

and

$$\int \text{cn}^4(\mathcal{B}) d\mathcal{B} = \left(2 - \frac{2}{m}\right) \int \text{cn}^2(\mathcal{B}) d\mathcal{B} - \frac{\mathcal{B}}{m^2} \left(\frac{4}{3} - \frac{7}{3}m + m^2\right) + \frac{2}{3} \cdot \frac{2 - m}{m^2} E(\text{am}(\mathcal{B}), m) + \frac{1}{3m} \text{cn}(\mathcal{B})\text{sn}(\mathcal{B})\text{dn}(\mathcal{B}).$$

Here $E(\cdot, m)$ represents the incomplete elliptic integral of the second kind and $\text{am}(\cdot, m)$ is the Jacobi amplitude function [36]. The above expressions imply

$$\int_{\mathcal{B}_0(0)}^{\mathcal{B}_0(t)} \text{cn}^2(\mathcal{B}) d\mathcal{B} = \mathcal{B}_0 - \frac{\mathcal{B}_0}{m} + \frac{E(\text{am}(\mathcal{B}_0), m)}{m},$$

and

$$\int_{\mathcal{B}_0(0)}^{\mathcal{B}_0(t)} \text{cn}^4(\mathcal{B}) d\mathcal{B} = \left(1 - \frac{5}{3m} + \frac{2}{3m^2}\right) \mathcal{B}_0 + \frac{2(2m - 1)}{3m^2} E(\text{am}(\mathcal{B}_0), m) + \frac{1}{3m} \text{cn}(\mathcal{B}_0)\text{sn}(\mathcal{B}_0)\text{dn}(\mathcal{B}_0).$$

Hence, the first and second terms of equation (54) are computed as

$$\int_0^t \left\{ \eta - \frac{1}{4}\eta^2 \right\} dt' = \left(f_2 - \frac{f_2^2}{4} \right) t - \frac{(f_1 - f_2)}{c(f_1 - f_3)^{1/2}} \sqrt{\frac{2 + (f_1 - f_3)}{6}} (2 - f_2) \left\{ \mathcal{B}_0 - \frac{\mathcal{B}_0}{m} + \frac{E(\text{am}(\mathcal{B}_0), m)}{m} \right\} + \frac{(f_1 - f_2)^2}{2c(f_1 - f_3)^{1/2}} \sqrt{\frac{2 + (f_1 - f_3)}{6}} \times \left\{ \left(1 - \frac{5}{3m} + \frac{2}{3m^2} \right) \mathcal{B}_0 + \frac{2(2m - 1)}{3m^2} E(\text{am}(\mathcal{B}_0), m) + \frac{1}{3m} \text{cn}(\mathcal{B}_0)\text{sn}(\mathcal{B}_0)\text{dn}(\mathcal{B}_0) \right\}, \quad (55)$$

and

$$\left\{ -\frac{1}{3c}\eta_x + \frac{\zeta_0^2}{2c}w_x \right\}_0^t = \frac{1}{c} \sqrt{\frac{6}{2 + (f_1 - f_3)}} (f_1 - f_2)(f_1 - f_3)^{1/2} \text{cn}(\mathcal{B}_0)\text{sn}(\mathcal{B}_0)\text{dn}(\mathcal{B}_0) \times \left\{ \frac{1}{3} + \frac{\zeta_0^2}{4} \left\{ - (2 - f_2) + (f_1 - f_2)\text{cn}^2(\mathcal{B}_0) + \frac{4}{2 + (f_1 - f_3)} \times (f_1 - f_3)(\text{dn}^2(\mathcal{B}_0) + m \text{cn}^2(\mathcal{B}_0) - m \text{sn}^2(\mathcal{B}_0)) \right\} \right\}. \quad (56)$$

Substituting equations (55) and (56) into equation (54), and treating the z -component of the particle location in a similar manner, the particle trajectories are given by the parametric curve

$$\begin{aligned} \bar{\xi}(t) - X_0 &= \left(f_2 - \frac{f_2^2}{4} \right) t - \frac{(f_1 - f_2)}{c(f_1 - f_3)^{1/2}} \sqrt{\frac{2 + (f_1 - f_3)}{6}} \times \\ & (2 - f_2) \left\{ \mathcal{B}_0 - \frac{\mathcal{B}_0}{m} + \frac{E(\text{am}(\mathcal{B}_0), m)}{m} \right\} + \frac{(f_1 - f_2)^2}{2c(f_1 - f_3)^{1/2}} \times \\ & \sqrt{\frac{2 + (f_1 - f_3)}{6}} \left\{ \left(1 - \frac{5}{3m} + \frac{2}{3m^2} \right) \mathcal{B}_0 + \frac{2(2m - 1)}{3m^2} \times \right. \\ & E(\text{am}(\mathcal{B}_0), m) + \frac{1}{3m} \text{cn}(\mathcal{B}_0)\text{sn}(\mathcal{B}_0)\text{dn}(\mathcal{B}_0) \left. \right\} + \frac{1}{c} \sqrt{\frac{6}{2 + (f_1 - f_3)}} \times \\ & (f_1 - f_2)(f_1 - f_3)^{1/2} \text{cn}(\mathcal{B}_0)\text{sn}(\mathcal{B}_0)\text{dn}(\mathcal{B}_0) \times \left\{ \frac{1}{3} + \frac{\zeta_0^2}{4} \left\{ - (2 \right. \right. \\ & - f_2) + (f_1 - f_2)\text{cn}^2(\mathcal{B}_0) + \frac{4}{2 + (f_1 - f_3)} (f_1 - f_3)(\text{dn}^2(\mathcal{B}_0) \\ & \left. \left. + m \text{cn}^2(\mathcal{B}_0) - m \text{sn}^2(\mathcal{B}_0)) \right\} \right\}, \end{aligned}$$

and

$$\begin{aligned} \bar{\zeta} - Z_0 &= \frac{\zeta_0}{c} \left\{ f_2 - \frac{1}{4}f_2^2 + (f_1 - f_2) \left(1 - \frac{f_2}{2} \right) \text{cn}^2(\mathcal{B}_0) \right. \\ & - \frac{1}{4}(f_1 - f_2)^2 \text{cn}^4(\mathcal{B}_0) + \frac{1}{2 + (f_1 - f_3)} (f_1 - f_2) \times \\ & (f_1 - f_3)[\text{sn}^2(\mathcal{B}_0)\text{dn}^2(\mathcal{B}_0) - \text{cn}^2(\mathcal{B}_0)\text{dn}^2(\mathcal{B}_0) \\ & \left. \left. + m \text{sn}^2(\mathcal{B}_0)\text{cn}^2(\mathcal{B}_0) \right] \right\}, \end{aligned}$$

where X_0 and Z_0 are constants that represent the variation between the initial positions of the particle and the relations on the right hand sides when analyzed at time $t = 0$ (that is, at $\mathcal{B}_0(0) = \frac{1}{2} \sqrt{\frac{6}{2 + (f_1 - f_3)}} (f_1 - f_3)^{1/2}(\xi_0)$). The

approximate analytical solution of the particle trajectories (33) and (34) which is connected to the solitary wave encounter the problem of horizontal excursion been underrated, the approximations for periodic waves are not exempted from this problem. As in the case of a solitary wave, direct integration was performed on differential equations (47) and (48) using the fourth-order Runge-Kutta method. In doing so, the equation for w must be used as seen in relations (52) and (53).

Now a few illustrations of particle trajectories will be given. The periodic traveling waves in the form where the trough of the wave corresponds to the undisturbed fluid surface is considered first. In Figure 5, the particle trajectories (ξ, ζ) for periodic waves for one complete cycle using the fourth-order RungeKutta method are shown. The closeup in the lower panel shows the importance of periodicity. It is seen that the particle accomplishes a small elliptic cycle prior to its up turning and riding into the next wave.

In Figure 6, a train of cnoidal waves is presented. A numerical solution of (47) and (48) is compared to the approximate trajectory $(\bar{\xi}, \bar{\zeta})$. The vertical speed and the total vertical excursion of the particles closer to the bed are smaller compared to others. It is also noticeable that the shorter particle trajectories are produced from the approximation $(\bar{\xi}, \bar{\zeta})$. This is pretty much the same as the results obtained for the particle trajectories below the solitary waves.

Lastly, Figure 7 presents the evolution of a particle trajectory in the surface of flow during several cycles of a periodic wave, while Figure 8 shows the evolution of a particle trajectory beneath the surface of a flow.

V. CONCLUSION

In this paper, the movement of the fluid particles beneath the surface wave has been studied using the BBM approximation. The exact solutions of the BBM model describe the behavior of the wave patterns at the fluid surface, and the relations that expressed the velocity field of the fluid beneath the surface are obtained while deriving the BBM equation. The velocity field which is connected to a surface wave is defined using the coupled ordinary differential equations from which the particle trajectories of the fluid were later found. One of the methods suitable for solving the given ordinary differential equations which govern the particle paths is direct numerical integration. However, a fourth-order Runge-Kutta method is used to compute the numerical solutions of these ordinary differential equations. Furthermore, the approximate analytical solutions are made available for comparison purposes. The behavior of the evolution of the particles in the fluid was explored via the passage of a solitary wave and a periodic traveling wave at the surface. In addition, we compute the mass flux via a surface solitary wave. The numerical integration seems to give better results in all the cases considered.

REFERENCES

- [1] S. Abbasbandy and A. Shirzadi, "The first integral method for modified benjamin–bona–mahony equation," *Communications in Nonlinear Science and Numerical Simulation*, vol. 15, no. 7, pp. 1759–1764, 2010.
- [2] W. Hereman, "Shallow water waves and solitary waves," *Mathematics of complexity and dynamical systems*, pp. 1520–1532, 2011.

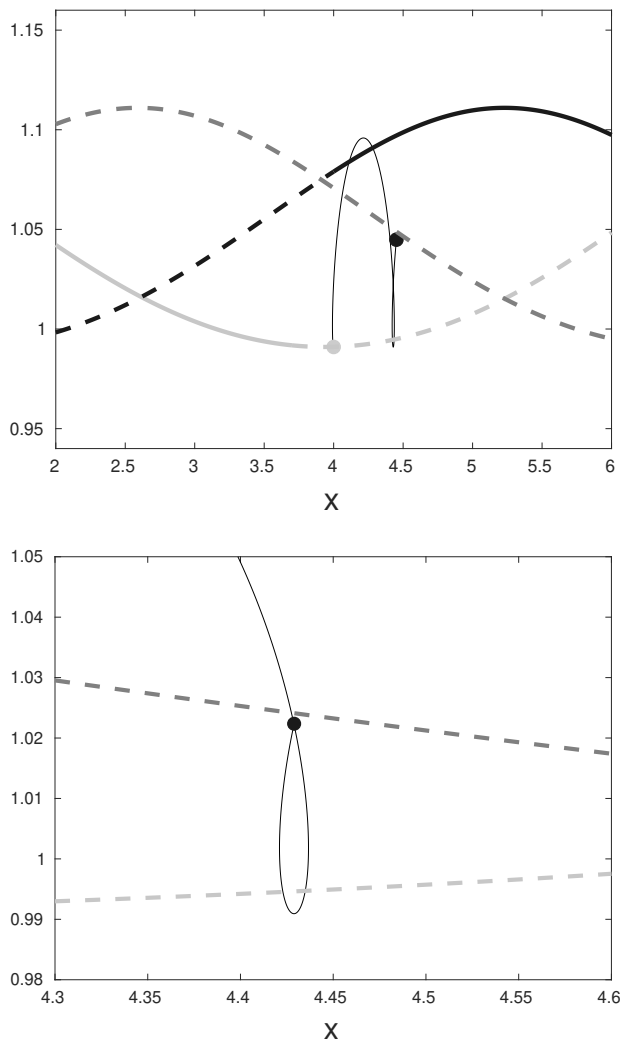


Fig. 5: The upper panel shows a periodic wave with wavelength 7.3208, period 7.6980 and phase speed $c = 0.9510$ at time $t = 0$ (light-gray), $t = 5$ (dark-gray) and $t = 10$ (black). The motion of the surface is indicated by the solid part which is kept constant in the curve. The path of a particle originated from $(x, z) = (4, 1)$ is shown. A close-up of the lower turning point is shown in the lower panel.

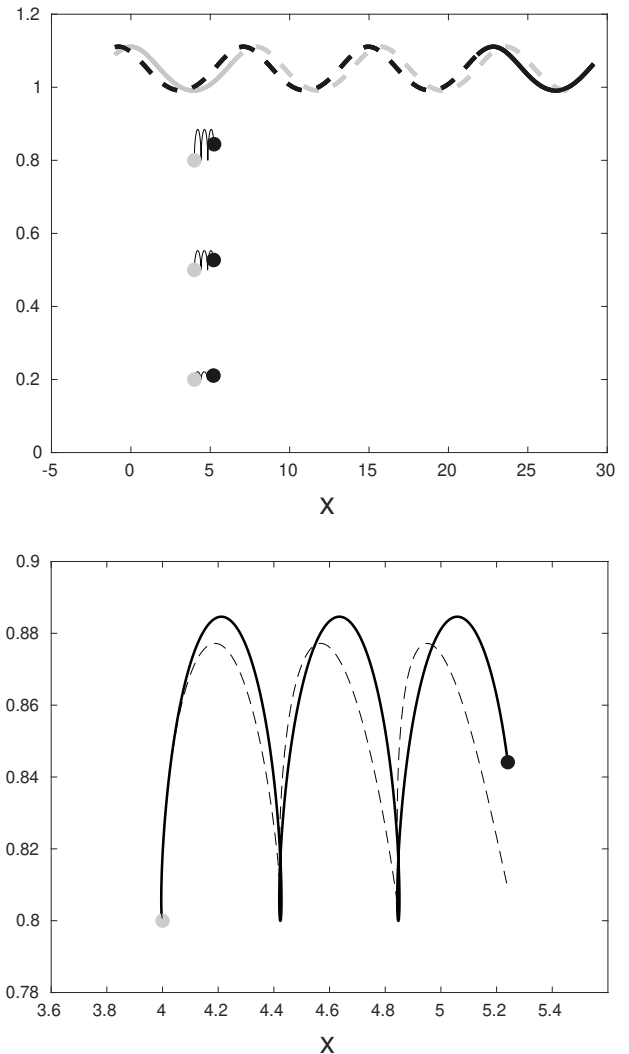


Fig. 6: The upper panel shows a periodic wave with wavelength 7.3208, period 7.6980 and phase speed $c = 0.9510$ at time $t = 0$ (light-gray) and $t = 24$ (black). The motion of the surface is indicated by the solid part which is kept constant in the curve. The paths of particles originally located at $(4, 0.8)$, $(4, 0.5)$ and $(4, 0.2)$ are shown. A close-up of the particle path initially positioned at $(4, 0.8)$ is shown in the lower panel, and the comparison with approximate path $(\bar{\xi}, \bar{\zeta})$ is indicated as a dashed curve.

[3] O. Ivanova, A. Aleksandrov, and R. Revetria, "Modelling of impact caused by flood after water flow optimization at volga-kama river basin." *Engineering Letters*, vol. 27, no. 4, pp. 658–662, 2019.

[4] K. S. Eke, O. F. Imaga, and O. Odetunmbi, "Convergence and stability of some modified iterative processes for a class of generalized contractive-like operators," *IAENG International Journal of Computer Science*, vol. 44, no. 4, pp. 587–590, 2017.

[5] J. Nickel, "Elliptic solutions to a generalized BBM equation," *Physics Letters A*, vol. 364, no. 3-4, pp. 221–226, 2007.

[6] D. Peregrine, "Calculations of the development of an undular bore," *Journal of Fluid Mechanics*, vol. 25, no. 2, pp. 321–330, 1966.

[7] D. Moldabayev, H. Kalisch, and D. Dutykh, "The Whitham equation as a model for surface water waves," *Physica D: Nonlinear Phenomena*, vol. 309, pp. 99–107, 2015.

[8] K. Singh, R. K. Gupta, and S. Kumar, "Benjamin–Bona–Mahony (BBM) equation with variable coefficients: similarity reductions and Painlevé analysis," *Applied Mathematics and Computation*, vol. 217, no. 16, pp. 7021–7027, 2011.

[9] T. B. Benjamin, J. L. Bona, and J. J. Mahony, "Model equations for long waves in nonlinear dispersive systems," *Philosophical Transactions of the Royal Society of London. Series A, Mathematical and Physical Sciences*, vol. 272, no. 1220, pp. 47–78, 1972.

[10] J.-C. Saut and N. Tzvetkov, "Global well-posedness for the KP-BBM equations," *Applied Mathematics Research Express*, vol. 2004, no. 1, pp. 1–16, 2004.

[11] V. Varlamov and Y. Liu, "Cauchy problem for the Ostrovsky equation," *Discrete & Continuous Dynamical Systems-A*, vol. 10, no. 3, pp. 731–753, 2004.

[12] M. A. Noor, K. I. Noor, A. Waheed, and E. A. Al-Said, "Some new solitary solutions of the modified Benjamin–Bona–Mahony equation," *Computers & Mathematics with Applications*, vol. 62, no. 4, pp. 2126–2131, 2011.

[13] A. A. Rady, E. Osman, and M. Khalfallah, "The homogeneous balance method and its application to the Benjamin–Bona–Mahony (BBM) equation," *Applied Mathematics and Computation*, vol. 217, no. 4, pp. 1385–1390, 2010.

[14] P. Estévez, Ş. Kuru, J. Negro, and L. Nieto, "Travelling wave solutions of the generalized Benjamin–Bona–Mahony equation," *Chaos, Solitons & Fractals*, vol. 40, no. 4, pp. 2031–2040, 2009.

[15] J.-Y. An and W.-G. Zhang, "Exact periodic solutions to generalized BBM equation and relevant conclusions," *Acta Mathematica Applicatae Sinica*, vol. 22, no. 3, pp. 509–516, 2006.

[16] S. D. Hatland and H. Kalisch, "Wave breaking in undular bores generated by a moving weir," *Physics of Fluids*, vol. 31, no. 3, p. 033601, 2019.

[17] M. K. Brun and H. Kalisch, "Convective wave breaking in the KdV equation," *Analysis and Mathematical Physics*, vol. 8, no. 1, pp. 57–75, 2018.

[18] J. D. Carter, C. W. Curtis, and H. Kalisch, "Particle trajectories in nonlinear schrödinger models," *Water Waves*, vol. 2, pp. 31–57, 2020.

[19] G. B. Whitham, *Linear and Nonlinear Waves*. Wiley, New York, 1974.

[20] A. Ali and H. Kalisch, "Energy balance for undular bores," *Comptes Rendus Mecanique*, vol. 338, no. 2, pp. 67–70, 2010.

[21] J. L. Bona, M. Chen, and J.-C. Saut, "Boussinesq equations and other systems for small-amplitude long waves in nonlinear dispersive media. i: Derivation and linear theory," *Journal of Nonlinear Science*, vol. 12, no. 4, pp. 283–318, 2002.

[22] H. Borluk and H. Kalisch, "Particle dynamics in the kdv approximation," *Wave Motion*, vol. 49, no. 8, pp. 691–709, 2012.

[23] A. Constantin and J. Escher, "Particle trajectories in solitary water waves," *Bulletin of the American Mathematical Society*, vol. 44, no. 3, pp. 423–431, 2007.

[24] A. Constantin, M. Ehrnström, and G. Villari, "Particle trajectories in linear deep-water waves," *Nonlinear Analysis: Real World Applications*, vol. 9, no. 4, pp. 1336–1344, 2008.

[25] A. Constantin and G. Villari, "Particle trajectories in linear water waves," *Journal of Mathematical Fluid Mechanics*, vol. 10, no. 1, pp. 1–18, 2008.

[26] M. Ehrnström and G. Villari, "Recent progress on particle trajectories in steady water waves," *Discrete Contin. Dyn. Syst. Ser. B*, vol. 12, no. 3, pp. 539–559, 2009.

[27] H.-K. Chang, Y.-Y. Chen, and J.-C. Liou, "Particle trajectories of nonlinear gravity waves in deep water," *Ocean Engineering*, vol. 36, no. 5, pp. 324–329, 2009.

[28] J. Fenton, "A ninth-order solution for the solitary wave," *Journal of fluid mechanics*, vol. 53, no. 2, pp. 257–271, 1972.

[29] R. Grimshaw, "The solitary wave in water of variable depth. part 2," *Journal of Fluid Mechanics*, vol. 46, no. 3, pp. 611–622, 1971.

[30] Y.-Y. Chen, H.-C. Hsu, and G.-Y. Chen, "Lagrangian experiment and solution for irrotational finite-amplitude progressive gravity waves at uniform depth," *Fluid dynamics research*, vol. 42, no. 4, p. 045511, 2010.

[31] J. Boussinesq, "Théorie des ondes et des remous qui se propagent le long d'un canal rectangulaire horizontal, en communiquant au liquide contenu dans ce canal des vitesses sensiblement pareilles de la surface au fond," *Journal de mathématiques pures et appliquées*, pp. 55–108, 1872.

[32] H. Kalisch and A. Senthikumar, "Derivation of boussinesq's shoaling law using a coupled bbm system," *Nonlinear Processes in Geophysics*, vol. 20, pp. 213–219, 2013.

[33] Z. Khorsand, "Particle trajectories in the serre equations," *Applied Mathematics and Computation*, vol. 230, pp. 35–42, 2014.

[34] A. Ali and H. Kalisch, "On the formulation of mass, momentum and energy conservation in the kdv equation," *Acta Applicandae Mathematicae*, vol. 133, no. 1, pp. 113–131, 2014.

[35] P. G. Drazin and R. S. Johnson, *Solitons: an introduction*. Cambridge university press, 1989, vol. 2.

[36] D. F. Lawden, *Elliptic functions and applications*. Springer, New York, 1989.

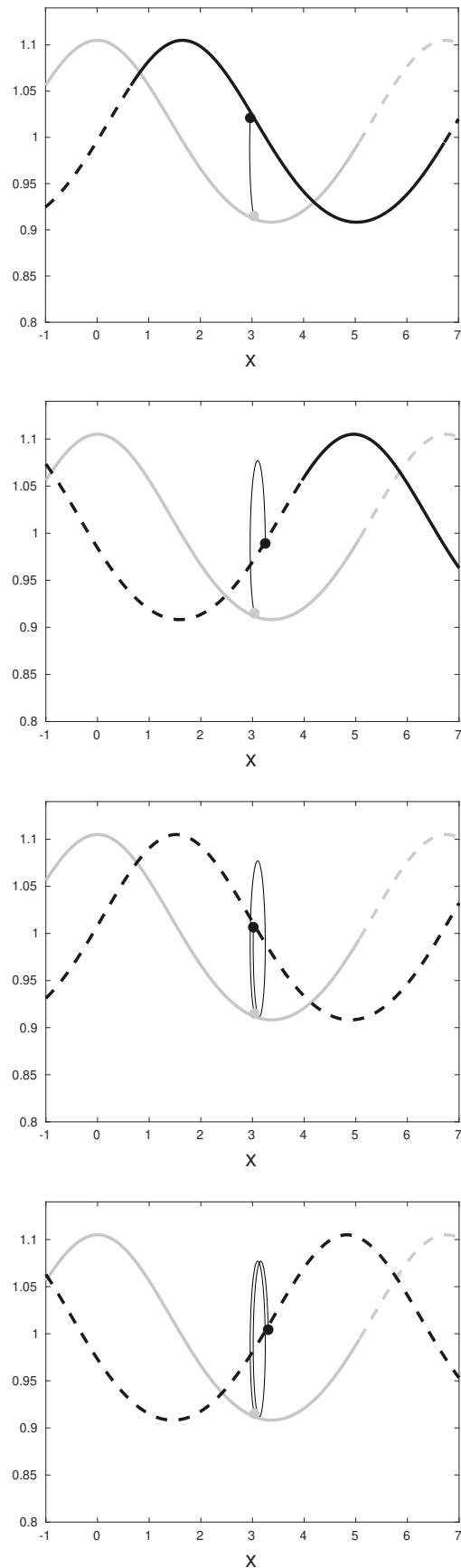


Fig. 7: A periodic wave with wavelength 6.0755, period 7.3499 and phase speed $c = 0.8266$ and mean zero is presented at $t = 0$ (light-gray) and $t = 2, t = 6, t = 10$ and $t = 14$ (black) in the upper panel, second to the upper panel, second to the lower panel and the lower panel, respectively. The motion of the surface is indicated by the solid part which is kept constant in the curve. The path of a particle originally located at (3.0368, 0.9150) is shown.

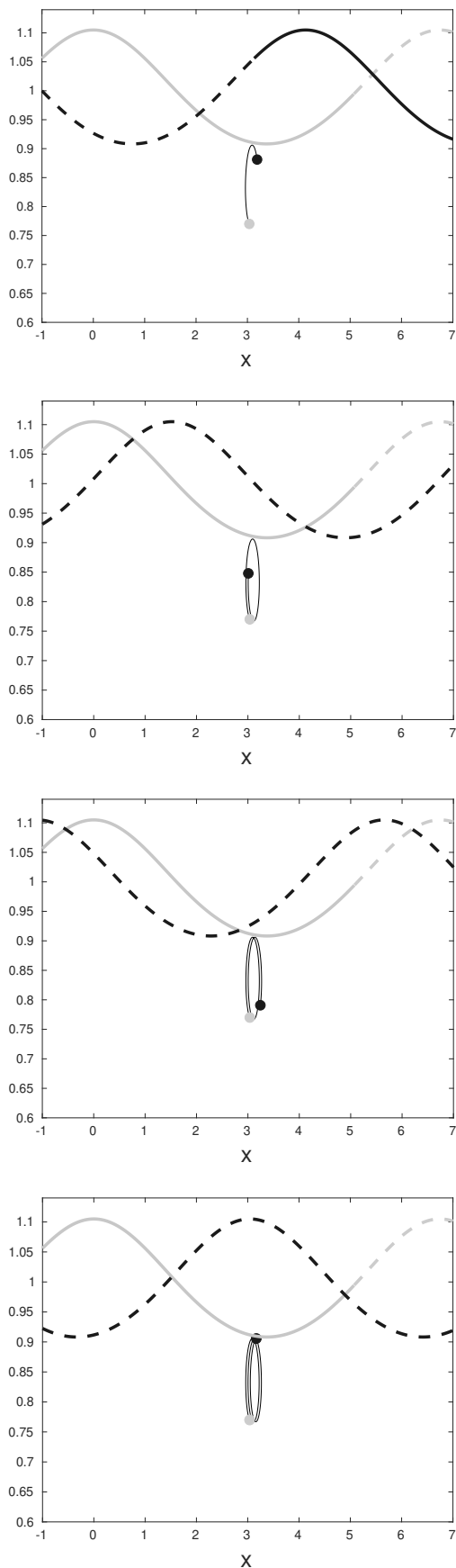


Fig. 8: A periodic wave with wavelength 6.0755, period 7.3499 and phase speed $c = 0.8266$ and mean zero is shown beneath the surface profile at $t = 0$ (light-gray) and $t = 5$, $t = 10$, $t = 15$ and $t = 20$ (black) in the upper panel, second to the upper panel, second to the lower panel and the lower panel, respectively. The motion of the surface is indicated by the solid part which is kept constant in the curve. The path of a particle originally located at (3.0368, 0.7700) is shown..